J|A|C|S

ARTICLES

Published on Web 01/24/2007

Infrared Spectroscopy of Cationized Arginine in the Gas Phase: Direct Evidence for the Transition from Nonzwitterionic to Zwitterionic Structure

Matthew F. Bush, Jeremy T. O'Brien, James S. Prell, Richard J. Saykally, and Evan R. Williams*

Contribution from the Department of Chemistry, University of California, Berkeley, California 94720-1460

Received August 31, 2006; E-mail: williams@cchem.berkeley.edu

Abstract: The gas-phase structures of protonated and alkali metal cationized arginine (Arg) and arginine methyl ester (ArgOMe) are investigated with infrared spectroscopy and *ab initio* calculations. Infrared spectra, measured in the hydrogen-stretch region, provide compelling evidence that arginine changes from its nonzwitterionic to zwitterionic form with increasing metal ion size, with the transition in structure occurring between lithium and sodium. For sodiated arginine, evidence for both forms is obtained from spectral deconvolution, although the zwitterionic form is predominant. Comparisons of the photodissociation spectra with spectra calculated for low-energy candidate structures provide additional insights into the detailed structures of these ions. Arg•Li^+, ArgOMe•Li^+, and ArgOMe•Na^+ exist in nonzwitterionic forms in which the metal ion is tricoordinated with the amino acid, whereas Arg•Na^+ and Arg•K^+ predominately exist in a zwitterionic form where the protonated side chain donates one hydrogen bond to the N terminus of the amino acid and the metal ion is bicoordinated with the carboxylate group. Arg•H^+ and ArgOMe•H^+ have protonated side chains that form the same interaction with the N terminus as zwitterionic, alkali metal cationized arginine, yet both are unambiguously determined to be nonzwitterionic. Calculations indicate that for clusters with protonated side chains, structures with two strong hydrogen bonds are lowest in energy, in disagreement with these experimental results. This study provides new detailed structural assignments and interpretations of previously observed fragmentation patterns for these ions.

Introduction

All naturally occurring amino acids are nonzwitterionic when isolated in the gas phase, despite existing as zwitterions in aqueous solutions over a wide pH range. The zwitterionic form of isolated glycine is not even a local minimum on the potential energy surface, and single-point energy calculations indicate that the zwitterionic form is 90 kJ/mol above the global minimum structure.[1] Attachment of a metal cation can preferentially stabilize zwitterionic forms of amino acids, with doubly charged cations typically having a greater effect than singly charged cations.[2−13] The nonzwitterionic form of glycine bound to a lithium ion is more stable than the zwitterionic form by only 13 kJ/mol, i.e., lithium ion adduction preferentially stabilizes the zwitterionic form by 77 kJ/mol.[2−4] Replacing the lithium ion with all but the smallest divalent alkaline earth metal, beryllium, makes the zwitterionic form of glycine lowest in energy.[4−6]

The proton affinity of the proton-accepting group can contribute to gas-phase zwitterion stablity.[14−19] For select sodiated amino acids with aliphatic side chains, the stability of the zwitterionic form relative to the nonzwitterionic form is directly related to proton affinity.[14,15] This relationship can be far less direct for non-aliphatic amino acids; heteroatoms in the side chain of basic residues can also solvate the metal ion, resulting in a substantial stabilization of the nonzwitterionic form of the amino acid.[20−23] For example, the proton affinity of lysine

(1) Kassab, E.; Langlet, J.; Evleth, E.; Akacem, Y. *J. Mol. Struct. (THEOCHEM)* **2000**, *531*, 267−282.
(2) Jensen, F. *J. Am. Chem. Soc.* **1992**, *114*, 9533−9537.
(3) Hoyau, S.; Ohanessian, G. *Chem.−Eur. J.* **1998**, *4*, 1561−1569.
(4) Hoyau, S.; Pelicier, J. P.; Rogalewicz, F.; Hoppilliard, Y.; Ohanessian, G. *Eur. J. Mass Spectrom.* **2001**, *7*, 303−311.
(5) Strittmatter, E. F.; Lemoff, A. S.; Williams, E. R. *J. Phys. Chem. A* **2000**, *104*, 9793−9796.
(6) Ai, H. Q.; Bu, Y. X.; Li, P.; Zhang, C. *New J. Chem.* **2005**, *29*, 1540−1548.
(7) Remko, M.; Rode, B. M. *J. Phys. Chem. A* **2006**, *110*, 1960−1967.
(8) Jockusch, R. A.; Lemoff, A. S.; Williams, E. R. *J. Am. Chem. Soc.* **2001**, *123*, 12255−12265.
(9) Bertran, J.; Rodriguez-Santiago, L.; Sodupe, M. *J. Phys. Chem. B* **1999**, *103*, 2310−2317.
(10) Constantino, E.; Rodriguez-Santiago, L.; Sodupe, M.; Tortajada, J. *J. Phys. Chem. A* **2005**, *109*, 224−230.
(11) Ai, H. Q.; Bu, Y. X.; Li, P.; Li, Z. Q.; Hu, X. Q.; Chen, Z. D. *J. Phys. Org. Chem.* **2005**, *18*, 26−34.
(12) Ai, H. Q.; Bu, Y. X.; Han, K. L. *J. Chem. Phys.* **2003**, *118*, 10973−10985.
(13) Wong, C. H. S.; Siu, F. M.; Ma, N. L.; Tsang, C. W. *J. Mol. Struct. (THEOCHEM)* **2002**, *588*, 9−16.
(14) Lemoff, A. S.; Bush, M. F.; Williams, E. R. *J. Am. Chem. Soc.* **2003**, *125*, 13576−13584.
(15) Wyttenbach, T.; Witt, M.; Bowers, M. T. *J. Am. Chem. Soc.* **2000**, *122*, 3458−3464.
(16) Julian, R. R.; Jarrold, M. F. *J. Phys. Chem. A* **2004**, *108*, 10861−10864.
(17) Strittmatter, E. F.; Wong, R. L.; Williams, E. R. *J. Phys. Chem. A* **2000**, *104*, 10271−10279.
(18) Strittmatter, E. F.; Williams, E. R. *Int. J. Mass Spectrom.* **2001**, *212*, 287−300.
(19) Strittmatter, E. F.; Williams, E. R. *J. Phys. Chem. A* **2000**, *104*, 6069−6076.

10.1021/ja066335j CCC: $37.00

is 110 kJ/mol higher than that of glycine.[24] The nonzwitterionic forms of the lithiated lysine and lithiated glycine are 29[23] and 13[2−4] kJ/mol more stable than the zwitterionic forms, respectively. In contrast to the trends established for the aliphatic amino acid, the nonzwitterionic form of lithiated lysine is preferentially stabilized by ∼16 kJ/mol compared to that for glycine, despite the 110 kJ/mol higher proton affinity of lysine.

Although the zwitterionic and nonzwitterionic forms of isolated arginine are close in energy,[25−29] the nonzwitterionic form is calculated to be more stable by ∼15 kJ/mol,[27−29] a result consistent with the infrared spectrum of the isolated molecule measured by cavity ringdown spectroscopy.[30] Various studies have explored mechanisms to stabilize zwitterionic forms of arginine in the gas phase.[16,22,27,31−34] Jockusch et al. investigated the structure of arginine in a gas-phase complex with a proton or an alkali metal ion.[22] Calculations indicate that zwitterionic structures are increasingly stable relative to nonzwitterionic structures with increased metal size. The nonzwitterionic form is most stable for lithiated arginine, whereas zwitterionic structures are favored for arginine with sodium and larger metal ions. In comparison, Bowers and co-workers found that nonzwitterionic forms of glycine, alanine, and analogous molecules of these two amino acids are preferentially stabilized by larger cations.[15] Dissociation of lithiated and sodiated arginine results in the loss of a water molecule, whereas loss of an ammonia molecule occurs with larger metal ions.[22] These results indicate a change in the structure of arginine from its nonzwitterionic form to the zwitterionic form with increasing metal ion size.

Additional experiments have sought to establish the structures of charged arginine clusters with complimentary techniques. Wyttenbach et al. investigated cationized arginine using ion mobility mass spectrometry.[32] Experimentally measured cross sections for sodiated and cesiated arginine fell within the range of those calculated for both low-energy salt-bridge (in which arginine is zwitterionic) and charge-solvated (nonzwitterionic) structures. Thus, no definitive conclusions about the structure of these ions could be deduced from these experiments. Calculations on sodiated and rubidiated *N*-amidinoglycine, a small model molecule, indicate that the salt-bridge structure is more stable for that molecule. For protonated arginine, the structure could not be unambiguously determined, although the data were "most consistent with a salt-bridge structure." Dissociation experiments by Cerda and Wesdemiotis also indicate that potasiated and cesiated arginine are zwitterionic, whereas the amino acid adopts nonzwitterionic forms when in a complex with a lithium or sodium ion.[33] A complication to the interpretation of these kinetic method experiments is that the structure of the amino acid in a cationized heterodimer of the amino acid and the methyl ester of the amino acid may not be the same as that of the isolated, cationized amino acid. For example, analogous experiments suggest that lithiated proline is nonzwitterionic,[35] a result that clearly disagrees with *ab initio* calculations[35−39] and binding energies determined from guided ion beam[37,38] and BIRD[39] experiments. Bowen and co-workers recently reported a photoelectron spectrum of arginine with an excess electron indicating that arginine exists as a zwitterion in that cluster.[31] This is consistent with calculations by Skurski et al. that show that the addition of an excess electron stabilizes the zwitterionic form of arginine by 31 kJ/mol and the nonzwitterionic form by only 15 kJ/mol, making the zwitterionic form the new global minimum in their calculations.[26]

Julian and Jarrold recently reported calculations on the structures and stabilities of derivatives of arginine as a function of proton affinity.[16] Comparing arginine to derivatives with up to three additional methyl groups on the side chain reveals that each additional methyl group increases both the proton affinity and stability of the zwitterion relative to the nonzwitterion, making the zwitterionic form of each arginine derivative lower in energy than the corresponding nonzwitterionic form. Interestingly, the addition of a fourth methyl group to arginine further increases the proton affinity of the molecule, yet destabilizes the zwitterionic form relative to the nonzwitterionic form due to additional steric and hydrogen-bonding constraints, making the nonzwitterionic form lower in energy in than the zwitterionic form.

Recent studies have demonstrated the potential of vibrational spectroscopy to probe the structure of cationized amino acids in the gas phase. Kapota et al. probed the structure of sodiated glycine and proline, yielding infrared signatures for the nonzwitterionic and zwitterionic forms of cationized aliphatic amino acids, respectively.[40] Polfer et al. have investigated the structures of cationized amino acids with aromatic side chains. Nonzwitterionic structures in which the metal ion is coordinated with the N-terminal nitrogen, the carbonyl oxygen, and the aromatic ring were observed for tyrosine•K^+[41] and phenylalanine•M^+, M = Ag[42] and K.[41] This structure is also adopted by tryptophan•M^+, M = Ag and Li, whereas spectra for clusters containing larger metal ions (M = Na, K, Rb, and Cs) indicate the presence of a second nonzwitterionic population in which

(20) Lemoff, A. S.; Bush, M. F.; Wu, C. C.; Williams, E. R. *J. Am. Chem. Soc.* **2005**, *127*, 10276−10286.
(21) Lemoff, A. S.; Wu, C. C.; Bush, M. F.; Williams, E. R. *J. Phys. Chem. A* **2006**, *110*, 3662−3669.
(22) Jockusch, R. A.; Price, W. D.; Williams, E. R. *J. Phys. Chem. A* **1999**, *103*, 9266−9274.
(23) Lemoff, A. S.; Bush, M. F.; O'Brien, J. T.; Williams, E. R. *J. Phys. Chem. A* **2006**, *110*, 8433−8442.
(24) Hunter, E. P.; Lias, S. G. *J. Phys. Chem. Ref. Data* **1998**, *27*, 413−656.
(25) Price, W. D.; Jockusch, R. A.; Williams, E. R. *J. Am. Chem. Soc.* **1997**, *119*, 11988−11989.
(26) Skurski, P.; Rak, J.; Simons, J.; Gutowski, M. *J. Am. Chem. Soc.* **2001**, *123*, 11073−11074.
(27) Julian, R. R.; Beauchamp, J. L.; Goddard, W. A. *J. Phys. Chem. A* **2002**, *106*, 32−34.
(28) Gdanitz, R. J.; Cardoen, W.; Windus, T. L.; Simons, J. *J. Phys. Chem. A* **2004**, *108*, 515−518.
(29) Rak, J.; Skurski, P.; Simons, J.; Gutowski, M. *J. Am. Chem. Soc.* **2001**, *123*, 11695−11707.
(30) Chapo, C. J.; Paul, J. B.; Provencal, R. A.; Roth, K.; Saykally, R. J. *J. Am. Chem. Soc.* **1998**, *120*, 12956−12957.
(31) Xu, S. J.; Zheng, W. J.; Radisic, D.; Bowen, K. H. *J. Chem. Phys.* **2005**, *122*, 091103.
(32) Wyttenbach, T.; Witt, M.; Bowers, M. T. *Int. J. Mass Spectrom.* **1999**, *183*, 243−252.
(33) Cerda, B. A.; Wesdemiotis, C. *Analyst* **2000**, *125*, 657−660.
(34) Julian, R. R.; Hodyss, R.; Beauchamp, J. L. *J. Am. Chem. Soc.* **2001**, *123*, 3577−3583.
(35) Talley, J. M.; Cerda, B. A.; Ohanessian, G.; Wesdemiotis, C. *Chem.−Eur. J.* **2002**, *8*, 1377−1388.
(36) Marino, T.; Russo, N.; Toscano, M. *J. Phys. Chem. B* **2003**, *107*, 2588−2594.
(37) Moision, R. M.; Armentrout, P. B. *J. Phys. Chem. A* **2006**, *110*, 3933−3946.
(38) Ye, S. J.; Moision, R. M.; Armentrout, P. B. *Int. J. Mass Spectrom.* **2006**, *253*, 288−304.
(39) Lemoff, A. S.; Bush, M. F.; Williams, E. R. *J. Phys. Chem. A* **2005**, *109*, 1903−1910.
(40) Kapota, C.; Lemaire, J.; Maitre, P.; Ohanessian, G. *J. Am. Chem. Soc.* **2004**, *126*, 1836−1842.
(41) Polfer, N. C.; Paizs, B.; Snoek, L. C.; Compagnon, I.; Suhai, S.; Meijer, G.; von Helden, G.; Oomens, J. *J. Am. Chem. Soc.* **2005**, *127*, 8571−8579.
(42) Polfer, N. C.; Oomens, J.; Moore, D. T.; von Helden, G.; Meijer, G.; Dunbar, R. C. *J. Am. Chem. Soc.* **2006**, *128*, 517−525.

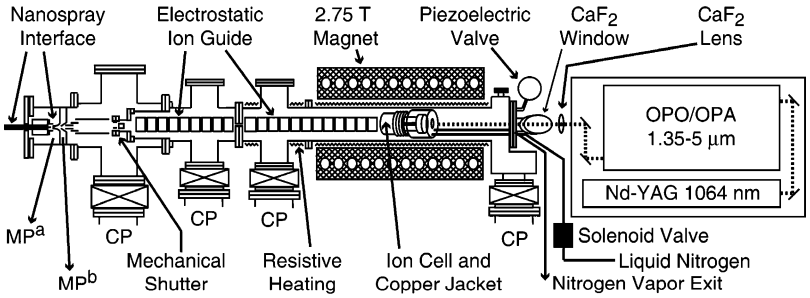

Figure 1. Schematic diagram of the Berkeley external nanospray ion source 2.75 T Fourier-transform ion cyclotron resonance mass spectrometer (side view) and tunable infrared laser system (top view). MP^a and MP^b are 8 and 24 L/s mechanical pumps, respectively, and CPs are 1500 L/s cryopumps. Detailed descriptions of the nanospray interface[47] and ion cell[48] are available elsewhere.

the metal ion coordinates with the carbonyl oxygen and the aromatic ring and in which the N terminus accepts a hydrogen bond from the carboxylic acid.[43] The relative size of this second population increases with metal ion size. These studies have made use of free electron lasers (CLIO[40] and FELIX[41−43]) and have been limited to wavelengths longer than 5 μm, precluding the observation of hydrogen stretches. As demonstrated by McLafferty and co-workers in their pioneering study of proton bound dimers of amino acids, table-top laser systems can be used to directly study hydrogen bonding in gas-phase amino acid clusters.[44] Kamariotis et al. recently reported hydrogen-stretch spectra of lithiated valine solvated by 1−4 water molecules.[45] From these experiments, information about the sites of initial solvation of the cluster and metal ion coordination are obtained. These spectra showed no evidence for zwitterionic structure.

Here, we report vibrational spectra of cationized arginine ($Arg{\bullet}M^+$, M = H, Li, Na, and K) and arginine methyl ester ($ArgOMe{\bullet}M^+$, M = H, Li, and Na) and results of complementary calculations that explore a wide range of zwitterionic and nonzwitterionic forms of these ions. These results provide direct experimental evidence that increasing metal ion size preferentially stabilizes the zwitterionic form of this amino acid. We find that $Arg{\bullet}Li^+$ is nonzwitterionic, whereas arginine in clusters with larger metal ions adopts a zwitterionic form. Although arginine in $Arg{\bullet}Na^+$ is predominately zwitterionic, a small fraction of the population is nonzwitterionic, and this may explain the unusual reactivity of this ion observed previously. In contrast to results from Bowers and co-workers that were most consistent with the zwitterionic form,[32] we find that protonated arginine is not zwitterionic.

Experimental and Theoretical Methods

Chemicals. The hydrochloride salt of arginine (Arg) and the dihydrochloride salt of arginine methyl ester (ArgOMe) were obtained from Sigma Chemical Co. (St. Louis, MO) and Alfa Aesar (Ward Hill, MA), respectively. Lithium hydroxide was purchased from Aldrich Chemical Co. (Milwaukee, WI). Sodium hydroxide and potassium hydroxide were purchased from Fischer Scientific (Pittsburgh, PA). All chemicals were used without further purification. The compositions of the solutions were selected to optimize signal for the ion of interest. To produce $Arg{\bullet}M^+$, M = Li, Na, and K, solutions were typically 1 mM Arg and 3 mM M^+ in ultrapure water (18.2 MΩ and ≤4 ppb total organic content) from a Milli-Q Gradient water purification system (Millipore, Billerica, MA). Solutions to produce $ArgOMe{\bullet}M^+$, M = Li, Na, and K, were typically 1 mM ArgOMe and 3 mM M^+ in methanol (EMD Chemicals, Gibbstown, NJ). Solutions to generate $Arg{\bullet}H^+$ and $ArgOMe{\bullet}H^+$ were made similar to those for $Arg{\bullet}M^+$ and $ArgOMe{\bullet}M^+$, respectively, without the addition of any alkali metal salt.

Mass Spectrometry and Photodissociation. All experiments were performed on a 2.75 T Fourier-transform ion cyclotron resonance mass spectrometer (Figure 1). Data were acquired using the modular FT/ICR data acquisition system "MIDAS".[46] Proton and alkali metal cationized clusters of arginine and arginine methyl ester were formed by nanospray ionization using a home-built interface, described in detail elsewhere.[47] These ions are transferred to the ion cell via a series of electrostatic lenses through five stages of differential pumping and are accumulated for 3−6 s in a home-built cylindrical ion cell, described in detail elsewhere.[48] To enhance trapping and thermalization of the ions, dry N_2 gas is pulsed into the cell at a pressure $\sim 10^{-6}$ Torr using a piezoelectric valve.

A 3−8 s delay is used to allow residual gases to be pumped out and to ensure that the ions reach a steady-state internal energy. The temperature of the ion cell was controlled by resistively heating the vacuum chamber around the cell. Prior to all experiments, the cell temperature is allowed to equilibrate for more than 8 h to ensure that ions are exposed to a radiative energy field given by Planck's distribution law. Due to the time scale of this delay (seconds) and the low pressure in the ion cell after accumulation (pressures $<10^{-8}$ Torr are typically reached after ~2 s), the ions studied here are radiatively equilibrated with the surrounding instrument.[49] All temperatures were recorded from a thermocouple attached directly to the copper jacket surrounding the ion cell.

The cluster of interest is isolated using a stored waveform inverse Fourier transform. After isolation, clusters are irradiated for 30−60 s using tunable infrared light produced by an optical parametric oscillator/amplifier (OPO/OPA) system (LaserVision, Bellevue, WA) pumped by the fundamental of a Nd:YAG laser (~8 ns pulses generated at a 10 Hz repetition rate, yielding ~3.8 W, Continuum Surelight I-10, Santa Clara, CA). Laser power is gated using a TTL-triggered mechanical shutter inside the pump laser cavity. The idler component from the OPA is isolated using a stack of Brewster-angle mounted silicon plates, yielding 90−210 mW of light with ~3 cm^{-1} bandwidth over the frequency range used in these studies. This light is aligned with the ion cell using protected silver mirrors enclosed in a positive-pressure, dry nitrogen purge box containing calcium sulfate desiccant (W.A.

(43) Polfer, N. C.; Oomens, J.; Dunbar, R. C. *Phys. Chem. Chem. Phys.* **2006**, *8*, 2744−2751.
(44) Oh, H. B.; Lin, C.; Hwang, H. Y.; Zhai, H. L.; Breuker, K.; Zabrouskov, V.; Carpenter, B. K.; McLafferty, F. W. *J. Am. Chem. Soc.* **2005**, *127*, 4076−4083.
(45) Kamariotis, A.; Boyarkin, O. V.; Mercier, S. R.; Beck, R. D.; Bush, M. F.; Williams, E. R.; Rizzo, T. R. *J. Am. Chem. Soc.* **2006**, *128*, 905−916.
(46) Senko, M. W.; Canterbury, J. D.; Guan, S. H.; Marshall, A. G. *Rapid Comm. Mass Spectrom.* **1996**, *10*, 1839−1844.
(47) Bush, M. F.; Saykally, R. J.; Williams, E. R. *Int. J. Mass Spectrom.* **2006**, *253*, 256−262.
(48) Wong, R. L.; Paech, K.; Williams, E. R. *Int. J. Mass Spectrom.* **2004**, *232*, 59−66.
(49) Price, W. D.; Williams, E. R. *J. Phys. Chem. A* **1997**, *101*, 8844−8852.

Hammond Drierite Co. Ltd., Xenia, OH), and focused using a 1 m CaF_2 spherical lens placed ~130 cm from the center of the ion cell. Light enters the vacuum chamber through a Brewster-angle mounted CaF_2 window.

Computational Chemistry. Candidate low-energy structures of Arg•M^+, M = Li, Na, and K, were determined using a combination of conformational searching and chemical intuition. Initial structures were generated using Monte Carlo conformation searching with the MMFF94 force field using Macromodel 8.1 (Schrödinger, Inc., Portland, OR). For the initial search, no constraints were placed on the molecules and at least 10 000 conformations were generated. Additional candidate structures were generated through searches using the Amber94 force field or by substituting the metal ion in a structure identified in another Monte Carlo search.

After identifying low-energy structures, hybrid method density functional calculations (B3LYP) were performed using Jaguar v. 6.5 (Schrödinger, Inc., Portland, OR). Structures were fully optimized using the LACVP* and LACVP++** basis sets. These basis sets use an effective core potential for K and the 6−31G* and 6−31++G** basis sets for all lighter atoms in these calculations, respectively. Vibrational frequencies and intensities were calculated using numerical derivatives of the LACVP++** energy minimized Hessian. All frequencies were scaled by 0.95. This scaling factor was chosen to give good agreement between the experimental spectra and calculated harmonic frequencies. This factor is close to that used previously to scale very similar calculations that were employed in the interpretation of experimental infrared spectra of hydrated clusters of protonated and lithiated valine (0.956).[45] Structures were minimized to geometries yielding all positive frequency vibrational modes, indicating that these are all local-minima structures.

Initial geometries for Arg•H^+ were obtained from MP2 structures previously reported by Rak et al.[29] These structures were minimized and vibrational frequencies calculated using the density functional methods discussed above. The previously reported structures **P1**, **P2**, **P3**, **P4**, and **P5** correspond to structures **D**, **I**, **E**, **F**, and **G** in the present work. Structure **P6** (similar to structure **J** in the present work) and related structures generated in this study all minimized to structure **D**.

Unless otherwise stated, all energies are from B3LYP/LACVP++** calculations, include zero-point energy corrections, and are reported as both 0 K energies (left of slash) and free energies at the temperature of the relevant experiment (right of slash). Energy corrections are calculated using unscaled harmonic oscillators. Vibrational frequencies for calculated infrared spectra have been scaled by 0.95, as discussed above. To approximate some of the temperature effects in the photodissociation spectra, line spectra are convoluted using 20 cm^{-1} full width half max Lorentzian peak shapes.

Experimental Results

Photodissociation. Infrared photodissociation data are acquired by simultaneously measuring precursor and fragment ion intensities resulting from laser irradiation as a function of frequency. Under the conditions of these experiments, ions reach a well-characterized internal energy distribution that closely resembles a Boltzmann distribution prior to laser irradiation.[50] The cell temperatures were chosen to ensure that some blackbody infrared radiative dissociation (BIRD) occurs (corresponding to ~1−24% dissociation of the precursor for reaction times up to 60 s), so that the ion population has enough internal energy to readily dissociate upon laser irradiation at frequencies at which the ions readily absorb. This makes it possible to observe photodissociation of these relatively small ions resulting from the absorption of just a single photon, although multiple photons can be absorbed prior to dissociation as well.

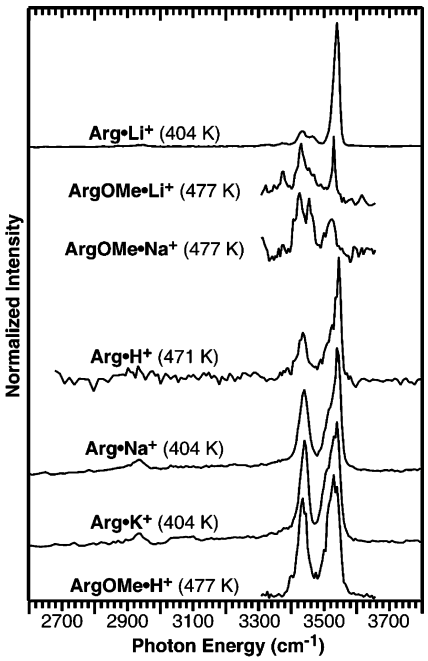

Figure 2. Experimental infrared photodissociation spectra of Arg•M^+, M = H, Li, Na, and K, and ArgOMe•M^+, M = H, Li, and Na. Copper jacket temperatures are marked on the respective experimental spectra. All spectra are corrected for background blackbody infrared radiative dissociation and laser power.

For Arg•M^+, M = H, Li, and Na, irradiation at the wavelengths investigated results exclusively in the loss of a water molecule, whereas for M = K, the loss of water and ammonia molecules are observed in a 1:3 ratio. The same product ions and branching ratios are observed with BIRD. Low-energy collisional activation produces the same fragment ions, but with slightly different relative abundances;[22] ~6% ammonia loss was observed for sodiated ions, and the loss of a water molecule for the potasiated species was weaker (~11%). For Arg•K^+, the branching ratio of ammonia and water loss does not depend on laser excitation frequency. For ArgOMe•M^+, M = H, Li, and Na, loss of a methanol molecule was the only fragmentation pathway observed.

Infrared Spectra. To obtain infrared photodissociation spectra, the background fragmentation due to BIRD must be subtracted from the laser photodissociation data. The BIRD kinetics are first order, as are the kinetics with laser irradiation. Therefore, the BIRD rates can be subtracted from the measured photodissociation rates to give the rates due to just the laser irradiation. An intensity value of zero corresponds to the signal observed in the absence of laser irradiation. The BIRD-corrected photodissociation rates are normalized for laser power by dividing the measured rate by the power of the laser at each frequency. This process produces a corrected photodissociation intensity (units $s^{-1}W^{-1}$) but does not correct for minor differences in dissociation efficiency resulting from different internal energy deposition as a result of the absorption of different energy photons.

The infrared photodissociation spectra obtained for Arg•M^+, M = H, Li, Na, and K, and ArgOMe•M^+, M = H, Li, and Na, are shown in Figure 2. Cell temperatures at which each of these spectra were acquired are indicated in the figure. The spectrum

(50) Price, W. D.; Schnier, P. D.; Jockusch, R. A.; Strittmatter, E. F.; Williams, E. R. *J. Am. Chem. Soc.* **1996**, *118*, 10640−10644.

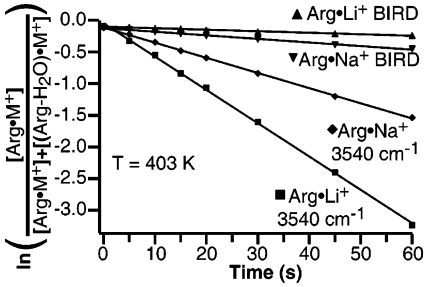

Figure 3. Blackbody and photofragmentation kinetics of Arg•Li^+ and Arg•Na^+ obtained at a copper jacket temperature of 403 K. Kinetic data were obtained with both species of interest present in the ion cell simultaneously and without isolation of the precursor ions.

for Arg•Li^+ is dominated by an intense band at 3540 cm^{-1} corresponding to the OH stretch of a carboxylic acid not involved in hydrogen bonding.[45] This is consistent with its disappearance in the spectrum of ArgOMe•Li^+, for which the carboxylic acid hydrogen is substituted by a methyl group. In contrast, the spectra for both sodiated and potasiated arginine are clearly different from those of the lithiated species.

Spectral Intensity. Although the higher frequency band for Arg•Na^+ and Arg•K^+ occurs at approximately the same frequency as that observed in the spectrum for Arg•Li^+, the relative intensity of the band is significantly greater in the spectrum of Arg•Li^+ than it is in any of the other spectra. The absolute intensity of a band in an action spectrum is related to the absorption cross section at a given wavelength, the laser flux ions are exposed to, the internal energy distribution of the precursor ions, the threshold dissociation energy of the ion, and other factors. The transition state entropy has a minimal effect for these relatively small ions under the conditions of this experiment.[49,50] The metal cationized arginine ions have different activation energies for dissociation. This affects the fraction of the ion population that is within one photon energy of the dissociation threshold. Thus, the absolute band intensities measured between spectra are not directly comparable in the absence of kinetic studies, such as those done for Arg•Li^+ and Arg•Na^+.

To determine the origin of the intensity difference for the high-frequency feature near 3540 cm^{-1} for Arg•Li^+ versus Arg•Na^+, BIRD and laser photodissociation kinetics at 3540 cm^{-1} were examined for these species (Figure 3). This frequency yielded the greatest photodissociation intensity in each of the respective experimental spectra. These data were acquired simultaneously with both ions in the cell to ensure that the ions are exposed to identical fluxes of both blackbody and laser radiation. These experiments were also done with and without precursor ion isolation to determine the effects of off-resonance excitation that can occur from ejecting all other ions from the cell. With conditions used in this specific experiment, ion isolation results in a reduction in the BIRD-corrected rate constant for photodissociation at 3540 cm^{-1} by 25 and 35% for lithiated and sodiated arginine, respectively. These results indicate that an isolation waveform can expand the ion cloud relative to the laser beam profile, although the effect is similar for both species in this case. Even if the diameter of the ion cloud is larger than that of the laser beam, magnetron motion can result in the entire population being exposed to equivalent laser power over the 300−600 pulses used in these experiments,[51] resulting in the ability to photodissociate at least 91% of the population with first-order dissociation kinetics.

From the data in Figure 3, it is clear that Arg•Li^+ is more thermally stable than Arg•Na^+, yet the rate constant for dissociation of Arg•Li^+ is twice that of Arg•Na^+ when both ions are simultaneously exposed to 3540 cm^{-1} photons. After correcting for BIRD, the photodissociation rate constant of Arg•Li^+ is ~3x greater than that of Arg•Na^+ at this frequency. The calculated internal energies at 404 K for the ten potential conformers of Arg•M^+ are all very similar and range from 56−59 and 58−61 kJ/mol for the lithiated and sodiated complexes, respectively. This indicates that the higher thermal stability of Arg•Li^+ versus Arg•Na^+ is due to a higher activation energy for dissociation for the former ion. For ions that are not in the rapid energy exchange limit, the relative thermal stability can be related to a relative activation energy for dissociation when the integrated infrared radiative absorption cross sections over a black body distribution are similar, as should be the case for these two ions.[52] Therefore, the substantially higher photodissociation rate measured at 3540 cm^{-1} is due to a much higher absorbance cross section for Arg•Li^+. Because the free acid stretches for these ions are calculated to have similar integrated absorption strengths (133 and 138 km/mol for Arg•Li^+ and 124 and 129 km/mol for Arg•Na^+), the substantial difference in intensity at 3540 cm^{-1} for the lithiated and sodiated ions must be due to a difference in structure; i.e., the spectra for the sodiated and potasiated clusters do not have a substantial contribution from a free carboxylic acid hydrogen stretch.

The acid OH stretch in the photodissociation spectrum of protonated arginine at 3545 cm^{-1} is slightly blue-shifted from that for Arg•Li^+, presumably due to the effects of the protonated side chain. Somewhat surprisingly, this band is significantly more intense relative to other bands for lithiated arginine versus protonated arginine. A weaker band is observed slightly below this frequency in the protonated methyl ester.

These results provide strong evidence that Arg•Li^+ is nonzwitterionic and that a major structural change occurs for the larger cations, consistent with a predominately zwitterionic form. Results for protonated arginine indicate a nonzwitterionic structure. Further interpretation of these spectra is enhanced by comparisons to spectra calculated for candidate low-energy structures, which are discussed in detail below.

Computational Results

Structural Families. Results from extensive conformational searching and *ab initio* calculations indicate that there are three low-energy nonzwitterionic (**A**−**C**) and seven low-energy zwitterionic (**D**−**J**) families of cationized arginine. The structure of the sodiated form of each family and the energy relative to the global minimum for each of the cationizing species are shown in Figure 4. The 0 K energies and free energies at 404 K of each family relative to the lowest-energy nonzwitterionic family (**A**) are plotted as a function of metal ion size in Figure 5 and Supplemental Figure 1 (see Supporting Information), respectively. These results show that zwitterionic structures are preferentially stabilized with increasing metal ion size, consistent with previous calculations.[22] In addition, trends in the relative stabilities of these structures as a function of metal ion size can be related to classes of structures that share very similar metal

(51) Jockusch, R. A.; Paech, K.; Williams, E. R. *J. Phys. Chem. A* **2000**, *104*, 3188−3196.
(52) Price, W. D.; Schnier, P. D.; Williams, E. R. *J. Phys. Chem. B* **1997**, *101*, 664−673.

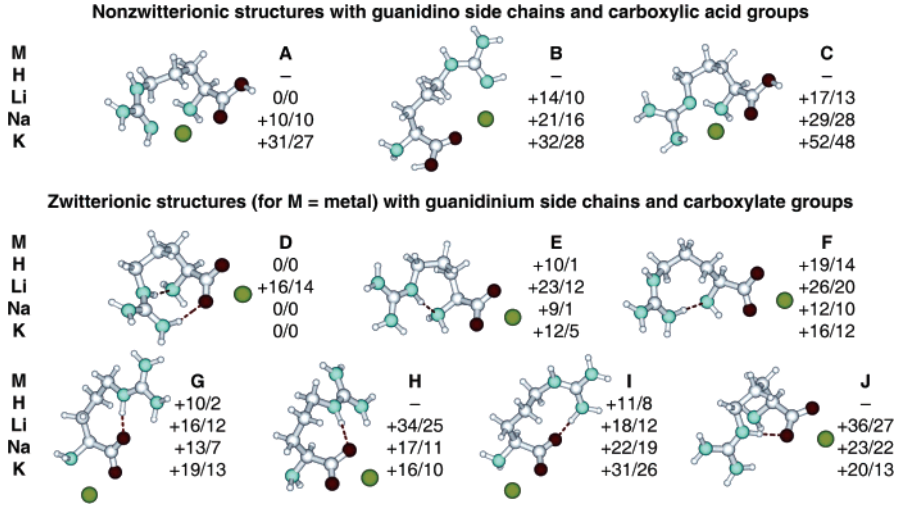

Figure 4. Energy minimized structures of the nonzwitterionic and zwitterionic forms of Arg•Na^+ from B3LYP/LACVP++** calculations. Zero-point energy corrected 0 K energies (left of slash) and free energies at the temperatures of the relevant experiments (right of slash) are in kJ/mol and reported relative to the lowest-energy structures for Arg•Na^+ and analogous Arg•M^+, M = H, Li, and K, ions with similar structures. Arg•H^+ structures, have protonated side chains and despite being exclusively nonzwitterionic, are compared to the zwitterionic, metal-cationized structures with similar hydrogen bonds.

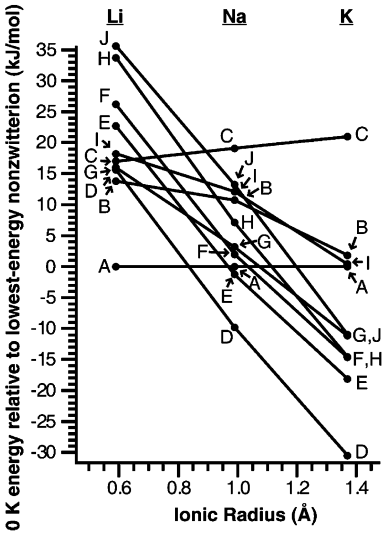

Figure 5. B3LYP/LACVP++** 0 K (zero-point energy corrected) energies of Arg•M^+, M = Li, Na, and K, relative to that of the lowest-energy nonzwitterionic structure (**A**). Free energies at 404 K of Arg•M^+, M = Li, Na, and K, relative to that of the lowest-energy nonzwitterionic structure (**A**) are shown in Supplemental Figure 1 (see Supporting Information).

ion binding motifs: $N_{SC}N_TO$ (**A** and **C**), $N_{SC}O$ (**B**), OO (**D**−**F**, **H**, and **J**), and N_TO (**G**, **I**), where N_T refers to the N-terminal nitrogen and N_{SC} refers to a nitrogen on the guanidino side chain.

Nonzwitterionic Forms. The lowest-energy nonzwitterionic structure for all alkali metal cationized arginine clusters studied here is **A**, in which the metal ion is coordinated by the N-terminal nitrogen, a η-nitrogen from the guanidino group, and the carbonyl oxygen ($N_{SC}N_TO$ coordinated). This structure is similar to the lowest-energy nonzwitterionic form of many aliphatic amino acids with smaller metal ions, which are typically N_TO coordinated,[8,14,53] and the lowest-energy form of lithiated lysine, in which the metal ion is also $N_{SC}N_TO$ coordinated.[23] **C** is also $N_{SC}N_TO$ coordinated, although the metal ion is solvated by the nitrogen in the ϵ position, not one of the two nitrogen atoms in the η position. This nonzwitterionic form (**C**) is on average 19 ± 2 kJ/mol higher in energy than **A** for the alkali metal containing ions. This value is obtained by averaging the differences between the zero-point energy corrected 0 K energies of **A** and **C** for each of the three metal ions and the uncertainty is the standard deviations of the three values. The average difference in free energies at 404 K is 17 ± 4 kJ/mol. Structure **B** becomes more similar in energy to **A** with increasing metal ion size, presumably because the hydrogen bond between the acid and the N terminus becomes a larger fraction of the stabilization energy in comparison to ion solvation. A similar structure was also identified for lithiated lysine,[23] and O-coordinated structures have been identified as local minima for many cationized aliphatic amino acids.[3,15,23]

Zwitterionic Forms. The lowest-energy zwitterionic form is **D**, a structure in which the metal ion is OO-coordinated and the side chain is protonated and donates hydrogen bonds to both the N terminus and an oxygen of the carboxylate group. Protonation of the N terminus is much less energetically favored. OO-coodination is a common metal ion binding configuration for the zwitterionic forms of cationized amino acids with aliphatic side chains[8,14,15,39] and is also present in the lowest-energy zwitterionic form of lithiated lysine[23] and lithiated and sodiated glutamine.[20] There are four additional structures with similar metal ion coordination that differ in the noncovalent interactions between the protonated side chain and the backbone of the amino acid. In **E**, the ϵ-NH group donates a hydrogen bond to the N-terminus, and the metal cationized structures in this family are 9 ± 3 kJ/mol (relative 0 K energies) and 1 ± 3 kJ/mol (relative $\Delta G_{404\ K}$) higher in energy than the corresponding structures in the **D** family. These values do not include data from the protonated structures. The inclusion of temperature corrections preferentially stabilizes structure **E** relative to structure **D** for these ions. Alternatively, when a η-NH_2 donates a hydrogen bond to the N-terminus (**F**), the structures are 13 ± 3 kJ/mol (relative 0 K energies) and 9 ± 3 kJ/mol (relative $\Delta G_{404\ K}$) higher in energy. In **H**, hydrogen atoms on the ϵ and η nitrogen atoms each interact with the carboxylate oxygen trans to the N terminus (17 ± 1 and 10.7 ± 0.4 kJ/mol higher in

(53) Lemoff, A. S.; Williams, E. R. *J. Am. Soc. Mass Spectrom.* **2004**, *15*, 1014−1024.

relative 0 K and $\Delta G_{404\ K}$ energies, respectively), whereas in **J**, these nitrogen atoms interact with the carboxylate oxygen cis to the N terminus (21 ± 2 and 16 ± 5 kJ/mol higher in relative 0 K and $\Delta G_{404\ K}$ energies, respectively). In both **H** and **J**, the ϵ-NH interacts more strongly with the oxygen than the η-NH_2.

In addition to zwitterions with OO-coordinated metal ions, cationized arginine can adopt zwitterionic forms with the metal N_TO coordinated, similar to the coordination previously found for low-energy nonzwitterionic amino acids, as discussed above. In **G**, hydrogen atoms on ϵ and η nitrogen atoms each interact with the carboxylate oxygen trans to the N terminus, whereas in **H**, only one hydrogen atom on a η-NH_2 group interacts with that carboxylate oxygen (8 ± 5 and 8 ± 7 kJ/mol higher in relative 0 K and $\Delta G_{404\ K}$ energies than the **G** structures, respectively).

Arginine Methyl Ester and Protonated Arginine. ArgOMe•M^+ structures were generated from structure **A**, for M = Li and Na, and **C**, for M = Li, of the analogous Arg•M^+ clusters. Structure **B** was not investigated because the loss of the hydrogen bond between the acid and N terminus makes this family energetically unfavorable. Structure **C** is 16.4 kJ/mol (relative 0 K energy) and 9.5 kJ/mol (relative $\Delta G_{404\ K}$) higher in energy than **A** for ArgOMe•Li^+, which is similar to energy differences between these structures of Arg•Li^+. A subsequent Monte Carlo conformational search of ArgOMe•M^+, M = Li, Na, and K, yielded no new structural families.

The side chains in both Arg•H^+ and ArgOMe•H^+ are protonated, like the zwitterionic form of alkali metal cationized arginine. The lowest-energy structure of Arg•H^+ (**D**) is very similar to the lowest-energy zwitterionic form found for Arg•M^+, M = Li, Na, and K, although structure **E** and **G** are within 2 kJ/mol with the inclusion of temperature corrections. Protonated structures analogous to the remaining OO-coordinated families (**H** and **J**) for cationized arginine are not stable at this level of theory. These same structures are the most stable for ArgOMe•H^+, although the electronic energies of structures **G** and **I** are ~40 kJ/mol higher than that of structure **D** at the B3LYP/LACVP* level of theory and were not evaluated further. For Arg•H^+, these structures have a hydrogen bond between the carboxylic acid and the N terminus that cannot be formed by the methyl ester of arginine. Zwitterionic structures of Arg•H^+, starting with **G** and **I**, but with both the side chain and N terminus protonated and the carboxylic acid deprotonated are not stable and minimize back to the respective nonzwitterionic forms. Note that protonated zwitterionic structures corresponding to **D**−**E** would have the two protonation sites immediately adjacent to each other and one less hydrogen bond, resulting in significant destabilization.

In summary, these density functional theory calculations indicate that arginine with a lithium cation attached is nonzwitterionic (**A**), but is zwitterionic (**D**) for the larger metal ions. For protonated arginine, the calculations indicate that the nonzwitterionic form (**D**) with the carboxylic acid not acting as a hydrogen bond donor is most stable. It should be noted that the relative energies of these structures depend on the level of theory, and on the harmonic potential approximation used to calculate frequencies for the zero-point energy and free energy corrections. In addition, it is possible that the absolute lowest-energy structures were not identified despite extensive conformational searching.

Discussion

Vibrational frequencies and intensities were calculated from the low-energy structures and compared to those measured experimentally. The free-OH and -NH stretch region in photodissociation spectra can be very indicative of structure. For example, the intensity of the free acid stretch in Val•$Li^+(H_2O)_3$ versus Val•$Li^+(H_2O)_2$ is significantly different and indicates a change in metal ion coordination.[45] In protonated water clusters, the relative intensities of bands associated with the dangling-OH stretches for double acceptor, single donor water molecules and those of single acceptor, single donor water molecules provide strong support for a water clathrate structure for $H^+(H_2O)_{21}$.[54−56] By comparison, information obtained from the presence (or absence) of bonded stretches can be more limited.

All calculated spectra contain several weak modes at frequencies between 2850 and 2950 cm^{-1}; seven for Arg•M^+ and ten for ArgOMe•M^+. These are CH stretching modes and are observed as a very weak photodissociation band centered near 3000 cm^{-1}. Because these weak modes are similar for all structures, the presence of this band provides limited structural information. It is interesting to note that the photodissociation yield in this frequency region is significantly less intense relative to the high-frequency bands than predicted computationally. This could be due to errors in the calculated intensities or differences between the absorbance cross sections and intensities in the action spectra. Some structures are calculated to have very strong modes in this region that are due to bonded NH stretches. Corresponding strong bands are not observed experimentally; this difference is discussed in more detail subsequently.

Structure of Arg•Li^+. The photodissociation spectrum for Arg•Li^+ along with the calculated spectra of candidate structures are shown in Figure 6. **A** and **C** are the only structures that have free (non-hydrogen bonding) acid stretches which have frequencies near 3540 cm^{-1}; hydrogen bonding, such as that in the nonzwitterionic structure **B**, shifts this most intense band to below 3100 cm^{-1}. Zwitterionic structures **D** and **G** do not have peaks corresponding to free acid stretches, although these structures have intense bands below 3300 cm^{-1} corresponding to bonded NH stretches of the side chain. Among the 10 conformers identified for Arg•Li^+, the photodissociation spectrum is most consistent with structure **A**, the calculated lowest-energy structure for this ion. In addition to the intense free acid stretch at 3542 cm^{-1}, the calculated spectrum has guanidino stretches at 3422 cm^{-1} (η-NH_2 symmetric stretch) and at 3458 cm^{-1} (ϵ-NH stretch) that are in very good agreement with the experimentally measured bands at 3430 and 3465 cm^{-1}. The η-NH_2 asymmetric stretch at 3534 cm^{-1} is likely obscured by the free-acid stretch. The only other structure that may contribute significantly to the photodissociation spectrum is **C**, the remaining structure with a free acid stretch, although the fit with this calculated spectrum is worse than that for structure **A**.

Structures of ArgOMe•Li^+ and ArgOMe•Na^+. Additional information about the structures of cationized arginine can be obtained by a comparison to the corresponding cationized methyl

(54) Miyazaki, M.; Fujii, A.; Ebata, T.; Mikami, N. *Science* **2004**, *304*, 1134−1137.
(55) Shin, J. W.; Hammer, N. I.; Diken, E. G.; Johnson, M. A.; Walters, R. S.; Jaeger, T. D.; Duncan, M. A.; Christie, R. A.; Jordan, K. D. *Science* **2004**, *304*, 1137−1140.
(56) Wu, C. C.; Lin, C. K.; Chang, H. C.; Jiang, J. C.; Kuo, J. L.; Klein, M. L. *J. Chem. Phys.* **2005**, *122*, 074315.

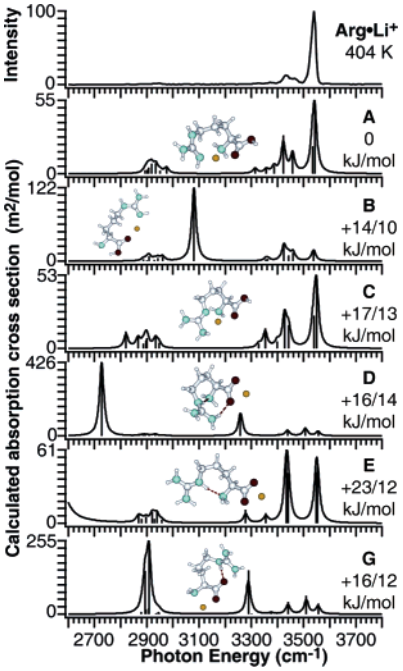

Figure 6. Infrared photodissociation spectrum of Arg•Li^+ obtained with a copper jacket temperature of 404 K and B3LYP/LACVP++** calculated vibrational spectra for the three lowest-energy Arg•Li^+ nonzwitterionic structures (**A**−**C**) and three low-energy zwitterionic structures (**D**, **E**, and **G**); 0 K energies (left of slash) and free energies at 404 K (right of slash) are reported relative to the lowest-energy structure (**A**). Calculated vibrational spectra for all structures are shown in Supplemental Figure 2 (see Supporting Information).

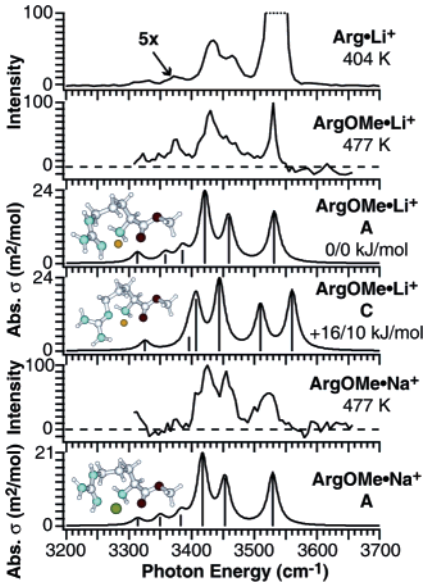

Figure 7. Infrared photodissociation spectra of Arg•Li^+, ArgOMe•Li^+, and ArgOMe•Na^+ and B3LYP/LACVP++** calculated vibrational spectra for structures **A** and **C** of ArgOMe•Li^+ and structure **A** of ArgOMe•Na^+. The spectrum for Arg•Li^+ has been expanded by a factor of 5 to show the lower intensity bands. Copper jacket temperatures are marked on the respective experimental spectra; 0 K energies (left of slash) and free energies at 477 K (right of slash) of ArgOMe•Li^+ are reported relative to the lowest-energy structure (**A**).

esters, which do not have acid stretches. Spectra for ArgOMe•Li^+ and ArgOMe•Na^+ are shown in Figure 7. Candidate low-energy structures for both these ions are also shown in this figure. For ArgOMe•Li^+, the peak at 3530 cm^{-1} corresponds to the η-NH_2 asymmetric stretch and is 10 cm^{-1} lower than the free acid

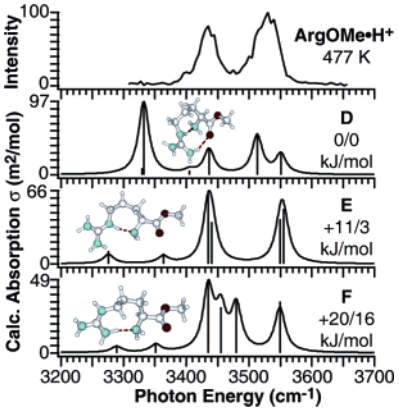

Figure 8. Infrared photodissociation spectrum of ArgOMe•H^+ obtained with a copper jacket temperature of 477 K and B3LYP/LACVP++** calculated vibrational spectra for the three lowest-energy ArgOMe•H^+ structures (**D**−**F**); 0 K energies (left of slash) and free energies at 477 K (right of slash) are reported relative to the lowest-energy structure (**D**).

stretch in Arg•Li^+ (3540 cm^{-1}); the latter is absent in the spectrum of the methyl ester. The fit to the lowest-energy structure **A** is better than to **C**. A band at 3460 cm^{-1} in the calculated spectrum is not observed as a distinct band in the measured spectrum, although there is significant photodissociation intensity in this region. The spectrum of ArgOMe•Na^+ is very similar to that of ArgOMe•Li^+ and is in very good agreement with that calculated for structure **A**. For ArgOMe•Na^+, the band at 3460 cm^{-1} is clearly present, but the corresponding band is not directly observed for the lithiated species. This may be attributable to any number of factors, including broadening of this mode, noise in the experimental spectrum, or the ion structure may be different from the identified low-energy structures.

Structures of Arg•Na^+, Arg•H^+, and ArgOMe•H^+. The photodissociation spectra for these clusters are similar to each other, but considerably different from the spectrum of Arg•Li^+. These spectra have common bands near 3440 cm^{-1} and 3540 cm^{-1}, although there are subtle differences between the spectra for the latter band.

Although ArgOMe•H^+ cannot adopt zwitterionic forms, the side chain of the amino acid is protonated and is calculated to have NH stretching modes similar to analogous stretches of zwitterionic metal cationized arginine. ArgOMe•H^+ has only three low-energy conformational families, versus five for protonated arginine and ten for metal cationized arginine, and the photodissociation cannot have contributions from OH stretching modes. Therefore, a detailed analysis of its spectrum (Figure 8) provides useful insights into the spectra of the other ions. Structure **E** is a better fit to the experimental data than either **D** or **F**. In this structure, the ϵ-NH donates a hydrogen bond to the N terminus of the amino acid backbone, neither η-NH_2 group interacts with the remainder of the cluster, and the symmetric stretch (3435 and 3441 cm^{-1}) and asymmetric stretch (3550 and 3555 cm^{-1}) modes for these two groups fall at nearly identical frequencies. When either η-NH_2 group donates hydrogen bonds, the positions of these modes are shifted, resulting in additional peaks in the spectrum (**D** and **F**).

The free acid stretch for Arg•H^+ occurs at a slightly higher frequency (~3545 cm^{-1}) than for Arg•Li^+, a result consistent with theory, which predicts a 13 cm^{-1} blue shift. The experi-

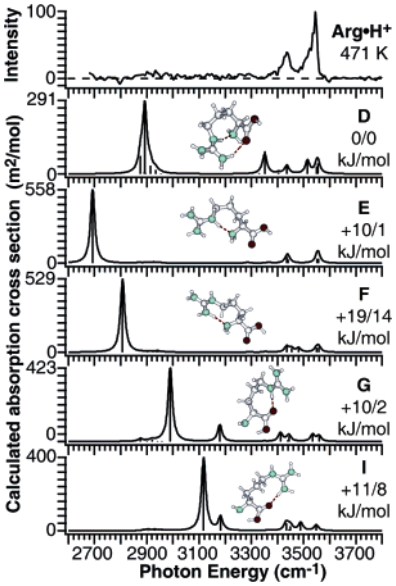

Figure 9. Infrared photodissociation spectrum of Arg•H^+ obtained with a copper jacket temperature of 471 K and B3LYP/LACVP++** calculated vibrational spectra for all low-energy Arg•H^+ structures (**D**−**G** and **I**). Zwitterionic structures of Arg•H^+ analogous to structures **G** and **I** were not calculated to be stable; 0 K energies (left of slash) and free energies at 471 K (right of slash) are reported relative to the lowest-energy structure (**D**).

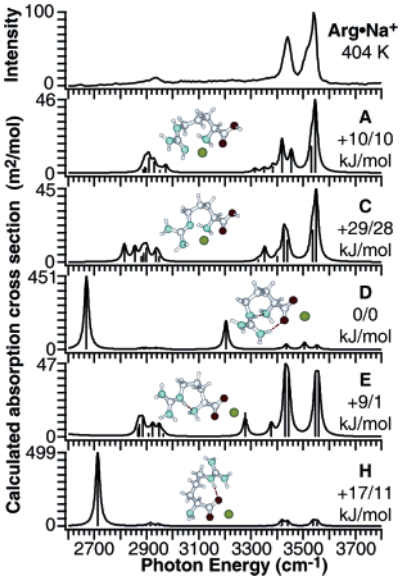

Figure 10. Infrared photodissociation spectrum of Arg•Na^+ obtained with a copper jacket temperature of 404 K and B3LYP/LACVP++** calculated vibrational spectra for two low-energy Arg•Na^+ nonzwitterionic structures (**A** and **C**) and three low-energy zwitterionic structures (**D**, **E**, and **H**); 0 K energies (left of slash) and free energies at 404 K (right of slash) are reported relative to the lowest-energy structure (**D**). Calculated vibrational spectra for all structures are shown in Supplemental Figure 3 (see Supporting Information).

mental spectrum and the spectra calculated for the five low-energy structures of Arg•H^+ are shown in Figure 9. No zwitterionic structures of protonated arginine analogous to structures **G** and **I** were calculated to be stable, so no direct comparison to calculated spectra for zwitterionic structures is made. However, if a zwitterion were formed by proton transfer from the carboxylic acid to the N terminus, one would not expect significantly more relative photodissociation at 3540 cm^{-1} (indicative of a free acid stretch) than is observed for ArgOMe•H^+. The high-frequency region of the spectrum is most consistent with that for **E**, which has bands similar to those discussed previously for ArgOMe•H^+, as well as an additional strong band for the free acid at 3554 cm^{-1}. The latter is superimposed on the asymmetric stretches of the η-NH_2 groups.

In the region below 3300 cm^{-1}, all calculated spectra have at least one intense band for bonded hydrogen stretches. This intense band is not observed in the experimental spectra over the frequency range measured. The calculated frequency of this band for **E** is near the low-frequency end of the experimental data, and it is possible that it appears at an even lower frequency. These calculated frequencies assume a scaled harmonic potential that may overestimate the frequency of this strongly bonded hydrogen stretch, which is likely to have significant anharmonic character.

The photodissociation spectrum of Arg•Na^+ (Figure 10) strongly resembles that of ArgOMe•H^+, suggesting that Arg•Na^+ has a protonated side chain and is therefore zwitterionic. However, the photodissociation spectrum of $ArgNa^+$ has an additional unresolved band at 3540 cm^{-1}, similar to, albeit less intense than, that observed for Arg•H^+. For Arg•H^+, this unresolved band is assigned to a free acid stretch that is at a similar frequency to the guanidinium asymmetric stretches assigned for ArgOMe•H^+. Unlike Arg•H^+, a single Arg•Na^+ structure cannot have both guanidinium stretches and a free acid stretch. This suggests that the Arg•Na^+ photodissociation spectrum is a composite of the spectra for at least two different conformers.

Calculated spectra for low-energy structures are compared to the experimental data in Figure 10. The photodissociation spectrum most resembles that of structures **E**, which has the same bands discussed ArgOMe•H^+ above, although structure **H** is also a reasonable fit. The photodissociation spectrum shows some similarity to that calculated for structure **A** as well. However, the calculated spectra for structure of **A** of Arg•Li^+ and Arg•Na^+ are very similar. If Arg•Na^+ were predominately structure **A**, we would expect that the experimentally measured spectrum would more closely resemble that of Arg•Li^+. Specifically, we would expect to resolve the two bands at 3430 and 3465 cm^{-1} where only one band is observed. Although the blue edge of the high-frequency band is indicative of a nonzwitterionic population with free acid stretches, i.e., structures **A** or **C**, the relatively low intensity of this band suggests that the population of the nonzwitterionic structure is small.

The photodissociation spectrum of Arg•Na^+ has broadband intensity below the free-NH stretching bands. This may be due to the symmetric stretching mode of the N_TH_2 group. When this group is a hydrogen-bond acceptor, such as in structures **E** and **F**, this group can in turn donate a strong hydrogen bond to the carboxylate group. This mode would be expected to be broad relative to the free-NH stretches.

Arg•Na^+ Spectral Deconvolution. To roughly estimate the relative populations that contribute to the photodissociation spectrum of Arg•Na^+, the free-NH/OH region of that spectrum was deconvoluted using a linear superposition of photodissociation spectra of references ions that model the zwitterionic and nonzwitterionic forms of Arg•Na^+. The photodissociation spectrum of Arg•Li^+, assigned to structure **A**, is used as a reference for nonzwitterionic Arg•Na^+ and that of ArgOMe•H^+, assigned to structure **E**, is used as a reference for zwitterionic

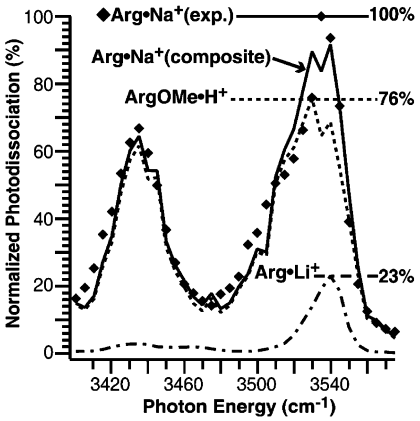

Figure 11. Photodissociation spectra for Arg•Li^+ and ArgOMe•H^+, which serve as reference spectra for the nonzwitterionic and zwitterionic forms of Arg•Na^+, respectively, are added to form a composite spectrum that closely resembles the experimental spectrum of Arg•Na^+ in this region.

Arg•Na^+. Note that even though ArgOMe•H^+ is not itself zwitterionic, it has a protonated side chain and serves as an excellent reference for the zwitterionic form **E** for alkali metal cationized arginine in this region. The calculated spectra for structure **A** of Arg•Na^+ and Arg•Li^+ are very similar in this region, as are those for structure **E** of Arg•Na^+ and ArgOMe•H^+.

Briefly, the spectra of Arg•Li^+, Arg•Na^+, and ArgOMe•H^+ were each normalized to yield the same intensity at the frequency of maximum photodissociation. The Arg•Na^+ spectrum was red-shifted by 5 cm^{-1} to better match the band positions for the other two clusters. Fractions of the photodissociation spectra for Arg•Li^+ (23% of the normalized Arg•Li^+ intensity) and ArgOMe•H^+ (76%) were added to yield a spectrum that is very similar to that measured for Arg•Na^+ (Figure 11). These fractions were obtained by minimizing the root-mean-square (rms) deviations between the composite and experimental spectra of Arg•Na^+. If the maximum cross sections contributing to the two component spectra were equal, this would indicate that about one forth of the Arg•Na^+ clusters are nonzwitterionic at 404 K and that the free energies of the zwitterionic and nonzwitterionic forms of Arg•Na^+ may differ by only 4 kJ/mol. However, this analysis overestimates the contribution of the nonzwitterionic form. On the basis of simultaneous photodissociation experiments (Figure 3) which indicate that the photodissociation yield of Arg•Li^+ is ~3 times higher than that of Arg•Na^+ at 3540 cm^{-1}, it is likely that the nonzwitterionic population is a factor of ~3 lower. Within the limits of the crude approximations of this deconvolution, this suggests that roughly 90% of the population is zwitterionic and that the nonzwitterionic form is ~8 kJ/mol higher in free energy, which is very similar to the 9 kJ/mol higher free energy for structure **A** relative to structure **E** at 404 K found computationally.

Structure of Arg•K^+. The experimental and calculated spectra for Arg•K^+ are shown in Figure 12 and are similar to those of Arg•Na^+, except that the blue edge of the highest-frequency band in the experimental spectrum is clearly less intense. This indicates that Arg•K^+ is predominately structure **E**, although structures **H** and **F** are also consistent with the photodissociation spectrum and cannot be ruled out. A composition analysis, as done for Arg•Na^+ using the ArgOMe•H^+ and Arg•Li^+ spectra as references for the zwitterionic form **E** and

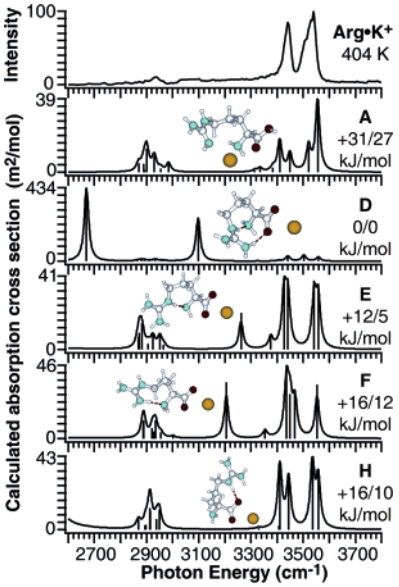

Figure 12. Infrared photodissociation spectrum of Arg•K^+ obtained with a copper jacket temperature of 404 K and B3LYP/LACVP++** calculated vibrational spectra for the lowest-energy nonzwitterionic structure (**A**) and four low-energy zwitterionic structures (**D**−**F**, and **H**) of Arg•K^+; 0 K energies (left of slash) and free energies at 404 K (right of slash) are reported relative to the lowest-energy structure (**D**). Calculated vibrational spectra for all structures are shown in Supplemental Figure 4 (see Supporting Information).

the nonzwitterionic form **A**, indicates that the Arg•K^+ spectrum is best fit by the ArgOMe•H^+ spectrum, exclusively (composites not shown for Arg•K^+). A variety of fits were performed where small frequency offsets were used to minimize rms deviations. In all cases, the fraction of Arg•Li^+ was small (−10% to +10%) and made only modest reductions to the rms deviation between the experimental and composite spectra. Although we are unable to accurately quantify the relative population of nonzwitterionic conformers, it is clear that the nonzwitterionic form must be far less populated relative to that observed for Arg•Na^+.

Calculations indicate that the free acid stretch in structure **A** is blue-shifted with increasing metal ions size (3542 and 3555 cm^{-1} for lithiated and sodiated arginine, respectively). This effect can clearly be seen in Figure 12 where this mode in structure **A** is at a significantly higher frequency than any observed features in the measured spectrum. In contrast, this band is aligned with the measured band for the lithiated ion (Figure 6). Combined, these results provide compelling experimental evidence that replacing Na with K in Arg•M^+ preferentially stabilizes the zwitterionic form relative to the nonzwitterionic form.

Relating Structure and Fragmentation for Metal Cationized Arginine. The structural change from a nonzwitterionic form to a zwitterionic form with increasing metal ion size is paralleled by a change in fragmentation from the loss of a water molecule to the loss of an ammonia molecule. Both theory and spectroscopic evidence indicate that this major structural change occurs between lithium and sodium. However, the major change in fragmentation pattern occurs between sodium and potassium. For Arg•K^+, for which both pathways are observed, the branching ratio for ammonia to water loss is larger for sustained off-resonance collisional activation (~10:1) than for BIRD and IR photodissociation with low laser power (~3:1). The internal energy deposition of the first is expected to be higher than the

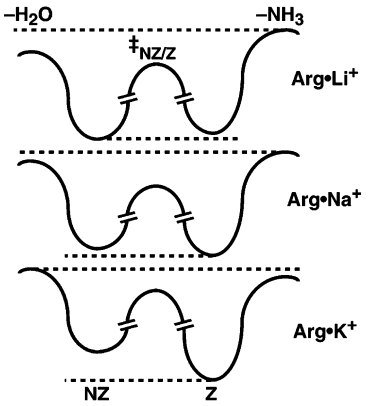

Figure 13. Conceptualized potential energy surfaces for structural isomerization between the nonzwitterionic (NZ) and zwitterionic (Z) forms of Arg•M^+, M = Li, Na, and K, and the loss of neutral molecules from the two forms of these ions. The surface for Arg•Na^+ illustrates how structural isomerization and water loss can be the major reaction pathway even thought the zwitterionic form is the predominate structure.

latter two methods, indicating that the loss of an ammonia molecule from the zwitterionic form of arginine is entropically favored. The appearance of both product ions indicates that the activation energies for both of these dissociation pathways are similar. However, the discrepancy between the change in fragmentation pathway and structural change as function of cation size indicates that the loss of an ammonia molecule has a slightly higher activation energy. For the zwitterionic form of arginine to lose a water molecule, as appears to be the case for Arg•Na^+ because only a small fraction the ion population is nonzwitterionic, the molecule must first rearrange to the nonzwitterionic form prior to dissociation (Figure 13).[22] This indicates that the isomerization barrier is below the dissociation barrier. As the zwitterionic form becomes preferentially stabilized with increasing cation size, the loss of an ammonia molecule becomes favored (Arg•K^+, Figure 13). For Arg•Na^+, loss of a water molecule occurs despite the predominately zwitterionic form because of structural isomerization and the slightly lower dissociation barrier for the loss of water compared to that for the loss of ammonia from the zwitterionic form.

Conclusions

The structures of cationized arginine have been investigated by a number of techniques. Infrared spectroscopy in the 2600−3800 cm^{-1} region, corresponding to hydrogen stretches, provides detailed structural information that has not been obtained by other methods. For alkali metal cationized arginine, a change in structure from nonzwitterionic to zwitterionic occurs with increasing metal ion size, with the transition occurring between lithium and sodium. Both forms of arginine in the sodiated species are observed, although the zwitterionic form is predominant. Protonated arginine is unambiguously determined to be nonzwitterionic.

A key advantage to these spectroscopic measurements is the ability to distinguish subtle differences in structure, a process enhanced by comparison to spectra calculated from candidate low-energy structures. For Arg•Li^+, ArgOMe•Li^+, and ArgOMe•Na^+, the measured spectra are excellent matches to those calculated for the lowest-energy structures determined from density functional theory. For Arg•Na^+, Arg•K^+, Arg•H^+, and ArgOMe•H^+, the experimental data are most consistent with structure **E**. For these ions, this structure is calculated to be 9−12 kJ/mol higher in energy at 0 K than the calculated lowest-energy structure (**D**), but is only 1−5 kJ/mol higher in energy after the inclusion of temperature corrections. Although the relative stabilities of **D** and **E** may be the result of the level of theory used, calculations with improved treatments of electron correlation by Rak et al. on protonated arginine[29] suggest that this is not the case. In their B3LYP/6−31++G** calculations, the electronic energy of structure **D** was found to be 13.4 kJ/mol more stable than structure **E**, a value that is directly comparable to the 13.3 kJ/mol difference for equivalent calculations in this work. This energy difference increases to 23.4 and 22.0 kJ/mol at the MP2/6−31++G** and CCSD/6−31++G**//MP2/6−31++G** level of theory, respectively. It is possible that the lowest-energy structure is not formed in these experiments, although this would not be anticipated under these experimental conditions, where there should be sufficient energy to overcome barriers to such minor structural changes. Future exploration of different theories would be interesting to pursue using these experimental results as a guide.

Acknowledgment. Generous financial support was provided by the National Science Foundation (Grants CHE-0415293 (ERW) and CHE-0404571 (RJS)) and the National Institutes of Health (Grant R01 GM064712-05 (ERW)). We thank Professor Alan G. Marshall and Dr. Gregory T. Blakney (National High Magnetic Field Laboratory) for the loan of, assistance with, and support for a modular FT/ICR data acquisition system (MIDAS) used in these studies.

Supporting Information Available: Cartesian coordinated for all structures and Supplemental Figures 1−4. This material is available free of charge via the Internet at http://pubs.acs.org.

JA066335J